Theoretical Study of the Mechanism and Rate Constant of the B + CO_2 Reaction

Benjamin Poully,[†,§] Astrid Bergeat,[‡,§] and Yacine Hannachi*[,†,§]

ISM Groupe de Spectroscopie Moléculaire and ISM Groupe d'Astrochimie, Université Bordeaux, Institut des Sciences Moléculaires (UMR 5255 CNRS), 351, cours de la Libération, F-33405 Talence cedex, France, and CNRS UMR 5255, ISM, Talence, France

Received: May 21, 2008; Revised Manuscript Received: July 7, 2008

The different stationary points on the potential energy surface relative to the title reaction have been reinvestigated at the B3LYP/aug-cc-pVDZ level with relative energies computed at the CCSD(T)/aug-cc-pVTZ level with B3LYP/aug-cc-pVDZ optimized geometries and by using the G3B3 composite method. Two entrance channels have been identified. The first one corresponds to boron addition at one of the oxygen atoms of the CO_2 molecule leading to *trans*-BOCO, which is found to be about 27 kcal/mol exothermic with a potential energy barrier of 16.4 kcal/mol (G3B3). The second channel, which has not been identified in previous theoretical works, corresponds to a direct insertion of the boron atom into a CO bond and leads to OBCO. The B + CO_2 → OBCO step is found to be about 84 kcal/mol exothermic and needs to overcome a potential energy barrier of only 3.6 kcal/mol (G3B3). The rate constant at 300 K of the insertion step, calculated by using TST theory with G3B3 calculated activation energy value, is 5.4 10^{-14} cm^3 $molecule^{-1}$ s^{-1}, in very good agreement with the experimental data ((7.0 ± 2.8) 10^{-14} cm^3 $molecule^{-1}$ s^{-1}, DiGiuseppe, T. G.; Davidovits, P. *J. Chem. Phys.* **1981**, *74*, 3287). The one corresponding to the addition process is found to be several orders of magnitude smaller because of a much higher potential energy barrier. The addition channel would not contribute to the title reaction even at high temperature. A modified Arrhenius equation has been fitted in the 300−1000 K temperature range, which might be useful for chemical models.

1. Introduction

The catalytic activation of carbon dioxide by metal centers has been extensively studied both experimentally and theoretically because it is considered as the key step in reducing the very thermodynamically stable carbon dioxide to useful organic molecules.[1−18] On the other hand, the reactions of boron atoms with small molecules have been only recently studied by using matrix isolation infrared spectroscopy and molecular beam methods coupled with mass spectroscopy or laser-induced fluorescence detection.[19−37] In the reaction of laser ablated boron atoms with CO_2 in a low temperature argon matrix, the insertion product, OBCO, was identified by its infrared fingerprint and confirmed by theoretical calculations.[19] To the best of our knowledge, only one experimental study has been performed in the gas phase on the B + CO_2 reaction.[38] By using a flow tube apparatus, the rate coefficient at 300 K was determined to be (7.0 ± 2.8) × 10^{-14} cm^3 $molecule^{-1}$ s^{-1}, CO_2 molecules being introduced in excess and boron atoms produced by a microwave discharge and detected by absorption at 249.7 nm. This rather slow measured rate coefficient shows that a sizable barrier is present in the entrance channel.

Marshall et al. conducted the first theoretical study of the title reaction at the UHF level with energies corrected at the MP2 level by using UHF optimized geometries.[39] Recently, Chin et al. reinvestigated theoretically this reaction at a more sophisticated level of theory.[40] The proposed reaction mechanism involves the addition of the boron atom to CO_2 producing *trans*-BOCO, which may dissociate to BO + CO ground states or isomerize to OBCO. The latter species may also dissociate to BO + CO. The transition structure of *trans*-BOCO dissociation was found to be lower in energy than that of the isomerization one leading to the conclusion that the observed OBCO species in matrix isolation experiments is produced by the recombination of BO and CO. However, the barrier height for the addition of the boron atom to CO_2 was found to be about 19 kcal/mol, which is not consistent with the measured rate constant at 300 K.[38] This discrepancy prompts us to reinvestigate the title reaction in order to examine if a more favorable entrance channel exists. Our study involves electronic structure calculations of the different stationary points on the potential energy surface, and the latter is used to obtain the rate constants of the different possible entrance channels. The computational methods are presented in the next section. Sections 3 and 4 report the results of our electronic structures and rate constants calculations, respectively. Finally, we present our conclusions in Section 5.

2. Computational Details

All calculations in the present study were performed by using the Gaussian03 program.[41] The stationary points on potential energy surfaces were located by using B3LYP density functional calculations,[42−44] with the aug-cc-pVDZ basis sets.[45,46] For each stationary point, we carried out single-point CCSD(T)/aug-cc-pVTZ//B3LYP/aug-cc-pVDZ energy calculations.[45−48] The correlation treatment in the coupled cluster calculations involved all valence electrons. The restricted and the unrestricted formalism are applied for closed-shell and open-shell systems respectively. The lowest-energy solution for each stationary point is obtained and verified through stability tests.[49,50] All located stationary points are on the $^2A'$ electronic state (when a symmetry plane exists). The lowest quartet state at the optimized

* Corresponding author: Fax (33) 5-40-00-66-45. E-mail: y.hannachi@ism.u-bordeaux1.fr.
† ISM Groupe de Spectroscopie Moléculaire, Université Bordeaux.
‡ ISM Groupe d'Astrochimie, Université Bordeaux.
§ ISM.

10.1021/jp804504g CCC: $40.75
Published on Web 08/13/2008

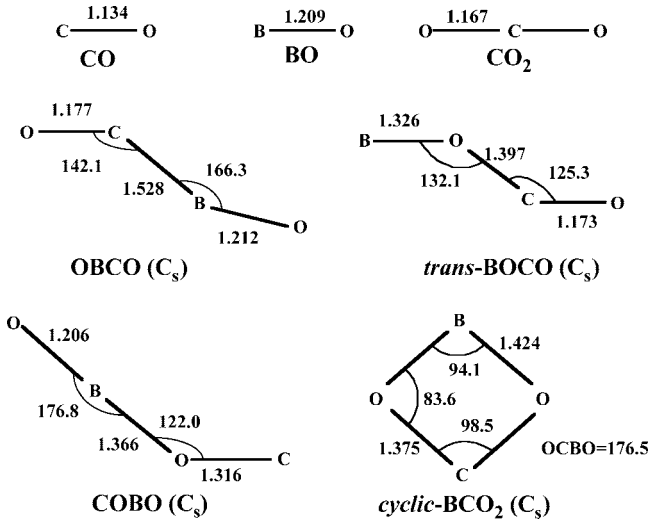

Figure 1. Optimized geometries of the various minima in the B + CO_2 reaction obtained at the B3LYP/aug-cc-pVDZ level (distances in angstroms and angles in degrees).

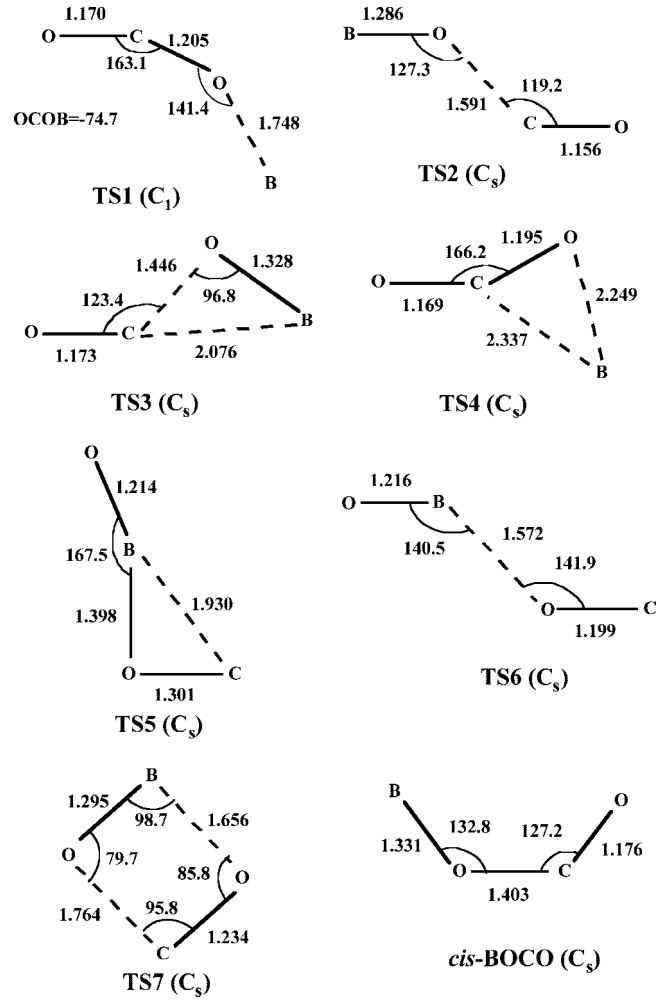

Figure 2. Optimized geometries of the various transition structures in the B + CO_2 reaction obtained at the B3LYP/aug-cc-pVDZ level (distances in angstroms and angles in degrees).

ground-state geometries (vertical excitation) is at least 58 kcal/mol higher in energy. The vibrational frequencies were calculated at the B3LYP/aug-cc-pVDZ levels for each stationary point and served to compute the zero point energies (ZPE, without scaling) and also to characterize the nature of the stationary points (minimum versus first-order saddle point). For CCSD(T) calculations, we applied the unscaled B3LYP/aug-cc-pVDZ ZPE corrections. In addition, we calculated the energies of the various stationary points on the potential energy surface by using the G3B3 composite model.[51] In order to verify whether the located transition structures connect the expected minima, intrinsic reaction coordinate (IRC) calculations[52] were carried out in both directions at the B3LYP/aug-cc-pVDZ level with a step size of 0.1 amu$^{1/2}$ bohr. The main transition structures have been reoptimized by using a wave-function-based method, namely, QCISD[48] with the aug-cc-pVDZ basis set and with a meta GGA functional, namely, MPW1B95[53] with the 6-31+G(d,p) basis set[54,55] in order to check whether it is not an artifact of B3LYP method. All reported energies are corrected for ZPE.

3. Results and Discussion

The optimized geometries of the different stationary points are shown in Figures 1 and 2. Figure 3 reports the schematic reaction mechanism with relative energies of the products, intermediate species, and transition structures obtained at the G3B3 levels. Table 1 reports the calculated relative energies obtained at the B3LYP, CCSD(T), and G3B3 levels of theory. The B3LYP harmonic vibrational frequencies of the various species involved in the title reaction are listed in Table 2.

3.1. Assessment of the Computational Methods. The calculated structural parameters of BO, CO, and CO_2, for which experimental data are available, are shown in Figure 1. There is a very good agreement between the calculated values and the corresponding experimental ones, 1.205 Å (BO), 1.128 Å (CO) and 1.162 Å (CO_2).[56,57] The nice agreement also holds for the vibrational frequencies. The calculated frequencies are 2185 cm^{-1} (CO), 1882 cm^{-1} (BO), and 667, 1354, and 2388 cm^{-1} (CO_2) (see Table 2). The corresponding experimental values are 2170 cm^{-1} (CO), 1895 cm^{-1} (BO), and 667, 1333, and 2349 cm^{-1} (CO_2).[56,57] The calculated B + CO_2 → BO + CO reaction energy is −61.0, −63.6, and −65.1 kcal/mol at the B3LYP, CCSD(T), and G3B3 level, respectively. The last two values are within the experimental uncertainties, −67 ± 5 kcal/mol, derived from the heat of formation of reactants and products.[58] The best value is obtained by using the composite G3B3 method. The energy difference between the BO ground state ($^2\Sigma^+$) and its first excited state ($^2\Pi$) is 65.1, 64.0, and 68.3 kcal/mol at the B3LYP, CCSD(T), and G3B3 level, respectively. Again, the best agreement with experiment[56] (68.1 kcal/mol) is achieved with the G3B3 method. Unless otherwise noted, the energetic values discussed below are those obtained with the G3B3 method.

3.2. Minima. Four minima, with CBO_2 stoichiometry, have been located on the potential energy surface. In agreement with previous studies, the lowest energy isomer is the insertion product OBCO (^{2}A′).[39,40] As shown in Figure 1, OBCO has a CO bond which is slightly stretched (0.01 Å) with respect to that of free CO_2. The BC bond length (1.528 Å) is consistent with that of a single bond. This species is calculated to be 83.9 kcal/mol lower in energy than the reactant ground states. The OBCO → BO ($^2\Sigma^+$) + CO ($^1\Sigma$) reaction energy is 18.8 kcal/mol. The next most stable species, COBO (^{2}A′), is calculated to be 36.3 kcal/mol higher in energy than OBCO and 47.6 kcal/mol lower in energy than the reactant ground states but 17.5 kcal/mol less stable than BO($^2\Sigma^+$) + CO($^1\Sigma$). This species has not been located in previous studies of the title reaction.[39,40] However, as we will see later, COBO is kinetically unstable and will be difficult to isolate in matrix isolation experiments. *Cyclic*-BCO_2 (^{2}A′) and *trans*-BOCO (^{2}A′) are much higher in

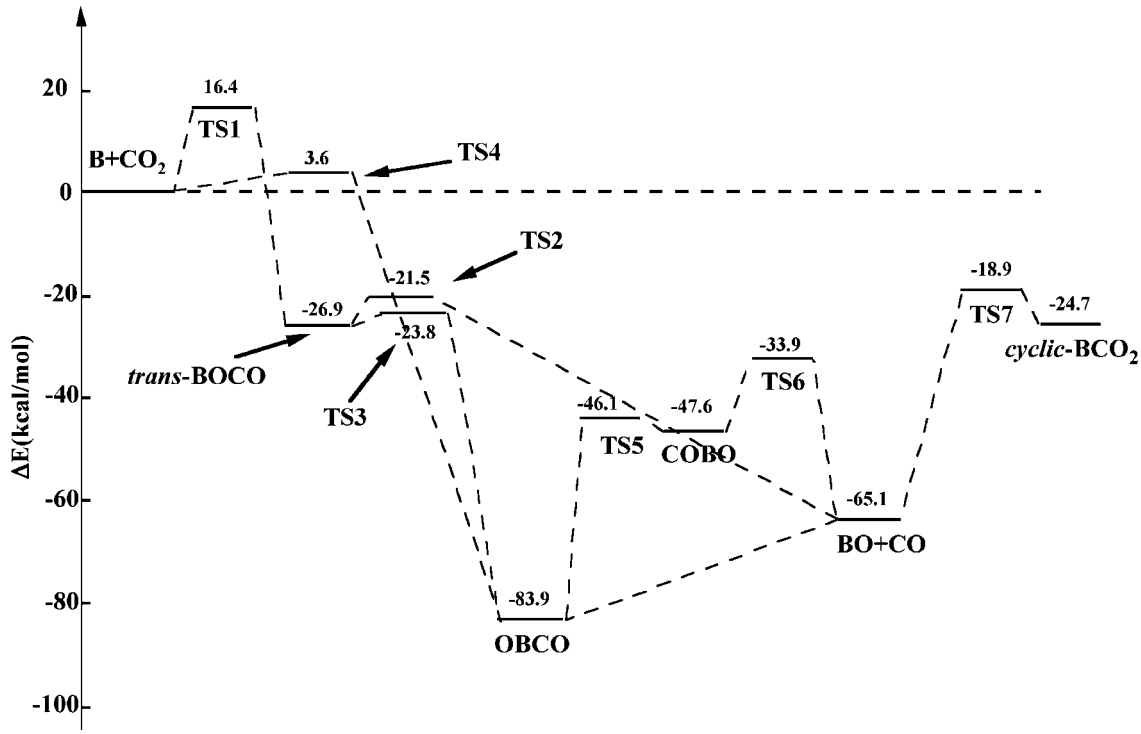

Figure 3. Schematic B + CO_2 reaction mechanism with G3B3 calculated relative energies (kcal/mol).

TABLE 1: Calculated Relative Energies (kcal/mol) Corrected for ZPE of the Various Compounds in the B + CO_2 Reaction

species	B3LYP	CCSD(T)	G3B3
B + CO_2	0.0	0.0	0.0
trans-BOCO	−27.2	−26.3	−26.9
OBCO	−86.8	−80.7	−83.9
COBO	−48.8	−45.8	−47.6
cyclic-BCO_2	−25.4	−25.9	−24.7
cis-BOCO	−25.2	−24.3	−25.0
TS1	11.2	16.8	16.4
TS2	−26.1	−21.3	−21.5
TS3	−24.3	−23.0	−23.8
TS4	2.7	4.5	3.6
TS5	−46.6	−44.4	−46.1
TS6	−38.6	−31.8	−33.9
TS7	−19.5	−19.1	−18.9
BO + CO	−61.0	−63.6	−65.1

TABLE 2: Calculated Vibrational Frequencies (cm^{-1}) of the Various Vompounds Obtained at the B3LYP/aug-cc-pVDZ Level

species	frequencies					
CO	2185					
BO	1882					
CO_2	667	667	1354	2389		
trans-BOCO	103	200	550	805	1272	1904
OBCO	200	268	470	679	1900	2034
COBO	166	449	513	873	1266	2048
cyclic-BCO_2	78	491	868	961	1145	1210
cis-BOCO	96i	163	579	770	1228	1873
TS1	788i	112	388	495	1106	2209
TS2	732i	82	164	432	1345	1976
TS3	365i	195	426	551	1301	1887
TS4	326i	146	499	581	1255	2255
TS5	359i	345	442	854	1319	1991
TS6	696i	102	238	451	1481	1854
TS7	487i	107	499	696	1436	1558

energy, 59.2 and 57 kcal/mol, respectively, less stable than OBCO. *Cis*-BOCO ($^2A'$), a first-order saddle point, is about 2 kcal/mol less stable than the trans isomer, and its imaginary frequency corresponds to torsion around the central CO bond, a motion that would lead to *trans*-BOCO.

3.3. Description of the Reaction Mechanism. As seen in Figure 3, two entrance channels have been identified. The reaction of a boron atom with carbon dioxide might produce *trans*-BOCO via the transition structure TS1, which is about 16 kcal/mol higher in energy than the reactant ground states. This value is lower than the one obtained in previous studies (19.2 kcal/mol).[40] TS1 has a BO bond length of 1.75 Å and a terminal CO bond virtually unchanged compared to free CO_2. The middle CO bond is stretched by 0.038 Å, and the OCO angle is bent to 163.1°. The TS1 transition structure has no symmetry (C_1) with an OCOB dihedral angle of −74.7°. The B + CO_2 → *trans*-BOCO reaction is 26.9 kcal/mol exothermic, similar to previous theoretical values reported by Marshall et al. (25.3 kcal/mol)[39] and by Chin et al. (25.1 kcal/mol).[40] IRC calculations confirm that TS1 connects separate reactants and *trans*-BOCO ($^2A'$). *Trans*-BOCO might rearrange to OBCO or dissociate to BO + CO, as has been found previously.[40] The dissociation to BO + CO, which proceeds via transition structure TS2, has an activation energy of 5.4 kcal/mol, a value which is higher than the value reported by Chin et al. (3.1 kcal/mol)[40] but closer to the earlier value of Marshall et al. (5 kcal/mol).[39] The central CO bond in TS2 is stretched by 0.194 Å to 1.591 Å, and the terminal CO and BO bonds are slightly shorter than in *trans*-BOCO. Again, IRC calculations confirm that TS2 connects *trans*-BOCO to BO + CO. The *trans*-BOCO → BO + CO reaction is 38.2 kcal/mol exothermic. The *trans*-BOCO → OBCO reaction step, in which the boron atom inserts into the adjacent CO bond, proceeds via transition structure TS3. In TS3, the BOC angle decreases to 96.8° (132.1° in *trans*-BOCO), and the CO bond, in which the insertion proceeds, is stretched to 1.446 Å. TS3 is lower in energy than TS2, 23.8 kcal/mol below the reactant ground states. It is interesting to note that the relative energy of TS2 and TS3 is very method dependent. G3B3 and CCSD(T) levels of theory put TS3 lower in energy

than TS2, whereas B3LYP gives the opposite situation. This was also the case in a previous work[40] where CCSD(T)/6-311G(d) and MP2/6-311G(d) at the B3LYP/6-311+G(d) optimized geometries put TS3 lower in energy, whereas B3LYP/6311+G(d), MP2/6311+G(3df)//B3LYP/6-311+G(d), and G2M(MP2) lead to a more stable TS2. The calculated energy difference is too small to enable us to draw a definitive conclusion. Nonetheless, as we will see later, this issue is not important in the title reaction.

The second entrance channel corresponds to a direct boron atom insertion into a CO bond of CO_2. The corresponding transition structure, TS4, is calculated to be only 3.6 kcal/mol higher in energy than the reactant ground states at the G3B3 level. The value obtained at the CCSD(T)/aug-cc-pVTZ, 4.5 kcal/mol, is larger. This transition structure has not been located in the more recent theoretical work on the title reaction.[40] A similar transition structure has been located in the work of Marshall et al. at the SCF level but assigned to *trans*-BOCO formation.[39] IRC calculations confirm that TS4 connects separate reactants to OBCO. The BO and BC bonds in TS4 are relatively long, 2.25 and 2.34 Å, respectively. The inserted CO bond is stretched by only 0.028 Å, and the OCO angle is bent to 166.2°. This is consistent with an early transition structure, in agreement with the exothermicity of the reaction.

Inspection of the IRC calculation at the B3LYP/aug-cc-pVDZ level shows that from B + CO_2 to TS4, there is little change of the CO_2 geometry as mentioned earlier (see the Supporting Information). The energy, the inserted CO bond, and the OCO angle start to change only when the BC bond length approaches 2.5 Å. After TS4 is passed, there is a simultaneous decrease of the BC and BO bond and an increase of the inserted CO bond. At the same time, the OCO angle decreases significantly. In this early part of the IRC, the energy also decreases significantly. The structure after this early step looks like an η^2_{co}-B(CO_2) complex similar to those found in transition-metal−CO_2 interaction.[1−3] Once the BC and BO bonds are formed, the CO bond which was initially just activated starts to break, and the CBO angle increases notably. The energy change in the latter part of the IRC is not as large as in the previous one. When the CO bond is completely broken, the CBO angle start to increase, and the BC is first somehow stretched then completely reformed until reaching the final structure of OBCO. The energy change in the last part of the IRC increases with respect to the previous one.

In order to check that TS4 is not an artifact of the B3LYP method, we carried out supplementary calculations on this species. First, we optimized the geometry and calculated the vibrational frequencies of the transition structure at the QCISD/aug-cc-pVDZ and MPW1B95/6-31+G(d,p). The obtained structure and vibrational characteristics of TS4 are very similar to those obtained by using B3LYP. We also ran IRC calculations at the MPW1B95/6-31+G(d,p) level, which confirmed that TS4 connects B + CO_2 to OBCO, in agreement with B3LYP.

From the insertion product OBCO, the reaction can proceed in two different pathways. A cleavage of the BC bond leads to BO + CO. This step is found to be 18.8 kcal/mol endothermic, as mentioned earlier. In order to check whether there is a transition structure connecting OBCO to BO + CO, we performed a relaxed scan of the potential energy surface along the BC bond. The energy increased smoothly from that of OBCO to that of BO + CO, showing that the reverse process BO + CO → OBCO reaction is barrierless. The second pathway from OBCO is the isomerization to COBO via a planar transition structure named TS5. The activation barrier of this step is 37.8 kcal/mol. TS5 is only 1.5 kcal/mol higher in energy than COBO, which makes the reverse reaction much faster. COBO can dissociate to BO + CO via transition structure TS6 with a potential energy barrier of 13.7 kcal/mol. In TS6, the central BO bond is stretched to 1.572 Å as compared to 1.366 Å in COBO. The COBO dissociation is 17.5 kcal/mol exothermic.

Finally, as in the previous work,[39,40] TS7, a transition structure connecting *cyclic*-BCO_2 to BO + CO, has also been located. The BO + CO → *cyclic*-BCO_2 reaction is calculated to be 40.4 kcal/mol endothermic with a barrier of 46.2 kcal/mol. The reverse reaction has a potential energy barrier of only 5.8 kcal/mol. We were not able to locate a transition structure connecting *cyclic*-BCO_2 and the other three minima on the CBO_2 potential energy surface or to B + CO_2 reactants. All our attempts converged to TS7 or to the other transition structures discussed previously. A transition structure connecting *cyclic*-BCO_2 to *cis*-BOCO has been located by Marshall et al. at the SCF/6-31G* level.[39] However, *cis*-BOCO is no longer a minimum in our work but a first-order saddle point as mentioned earlier.

We also considered alternative exit channel energetics. The B + CO_2 → BO($^2\Pi$) + CO($^1\Sigma$) reaction energy is found to be only 3.2 kcal/mol endothermic at the G3B3 level, which means that the first excited electronic state BO($^2\Pi$) might be populated. The other products are not easily accessible. C(^{3}P) + BO_2($^2\Pi_g$) is found to be 63.9 kcal/mol higher in energy than the reactant ground states. Finally, O(^{3}P) + BCO($^4\Sigma^+$) and O_2($^3\Sigma_g$) + BC($^4\Sigma$) are much higher in energy, 107.8 and 162.8 kcal/mol, respectively, above B + CO_2.

TABLE 3: Calculated Rotational Constants (B in cm^{-1}) Obtained at the B3LYP/aug-cc-pVDZ Level with Their Symmetries, σ, and Electronic Degeneracies, g_{el}

species		B/cm^{-1}		σ
CO_2	0.386	0.386		2
TS1	0.152	0.159	3.141	1
TS4	0.175	0.246	0.608	1

species	g_{el}	E/cm^{-1}	electronic states	
TS1 or TS4	2			
B	2[a]	0	$2s^12p^1$	$^2P°_{1/2}$
	4[a]	15.254[a]	$2s^12p^1$	$^2P°_{3/2}$

[a] Reference 60.

4. Rate Constant Calculations

The rate coefficient is calculated by transition state theory (TST) at a specified temperature, T,

$$k(T) = \frac{k_B T}{h} \frac{Q^{TS}}{Q^B Q^{CO_2}} g_{el} \exp\left(-\frac{E_0}{k_B T}\right)$$

where k_B and h are the Boltzmann and Planck constants, respectively, Q^{TS}, Q^B, and Q^{CO_2} are the partition functions per unit of volume (vibrational, rotational, and translational parts)[59] for the transition state, B, and CO_2, respectively, g_{el} is the ratio of effective electronic degeneracies of the transition state and the reactants, and E_0 is the energy of the transition state relative to that of the reactants when taking into account the ZPE of the species. The calculated parameters used are listed in Tables 2 and 3, with G3B3 calculated relative energies in Table 1. The rate coefficients, $k(T)$ for the reactions B + CO_2 → TS1 and TS4 calculated over the temperature range of 300−1000 K are showed in Figure 4 (calculated data are available in the Supporting Information for the insertion step). Because of the existence of the high reaction barrier, the channel via TS1

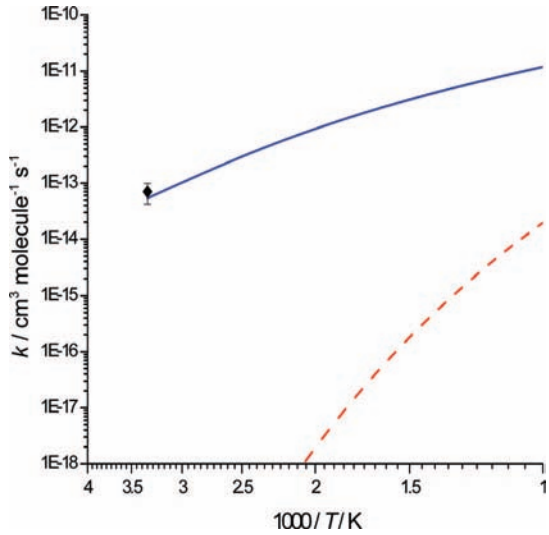

Figure 4. Arrhenius plots for the calculated rate coefficients, $k(T)$, for the reactions B + $CO_2 \xrightarrow{TS1}$ *trans*-BOCO (dashed line) and B + $CO_2 \xrightarrow{TS4}$ OBCO (full line). The experimental value at 300 K[38] is reported (square).

remains negligible: the most favorable pathway is B + $CO_2 \xrightarrow{TS4}$ OBCO→*BO* + CO .

The only experimental study in the gas phase of the B + CO_2 reaction gives a rate coefficient at 300 K of $(7.0 \pm 2.8) \times 10^{-14}$ cm^3 $molecule^{-1}$ s^{-1}. At this temperature, the rate coefficient calculated by TST is 5.4×10^{-14} cm^3 $molecule^{-1}$ s^{-1} with a G3B3 calculated relative energy E_0 which is in good agreement with the experimental values. The adjustment of the barrier height energy in order to fit the experimental rate coefficient value with its uncertainty at 300 K leads to $E_0 =$ 3.44 kcal mol^{-1}, which might be compared with the 3.6 kcal mol^{-1} calculated at the G3B3 level.

Because on an Arrhenious plot our calculated temperature dependence of the rate coefficient is not linear (see Figure 4), it may be represented in chemical models by using a modified Arrhenius equation.

$$k = A\left(\frac{T}{298}\right)^m \exp(-E/RT)$$

The three parameters A, m, and E have been derived from the nonlinear fitting of the above equation to the TST calculated results with the G3B3 energy in the temperature range 300−1000 K. The resulting values yield the following expression (in cm^3 $molecule^{-1}$ s^{-1}):

$$k = (1.64 \pm 0.02) \times 10^{-11}\left(\frac{T}{298}\right)^{1.154\pm0.005} \exp\left(-\frac{1725 \pm 4}{T}\right)$$

5. Summary and Conclusion

In the present work, the B + CO_2 reaction mechanism has been studied theoretically. Two entrance channels have been identified. The first one corresponds to the addition of the boron atom at an oxygen atom of carbon dioxide producing *trans*-BOCO, which is exothermic by approximately 27 kcal/mol. This species can isomerize to OBCO or dissociate to BO + CO in their ground states. The energy barrier involved in this entrance channel is predicted to be about 16 kcal/mol. A second much more favorable entrance channel corresponds to the direct boron atom insertion into CO_2 producing OBCO. This latter step is much more exothermic (85 kcal/mol) and involves an energy barrier of only 3.6 kcal/mol. The insertion species OBCO can also dissociate to BO + CO ground states. The reverse reaction BO + CO → OBCO is barrierless.

By taking into account the calculated rate constants of the two entrance channels, only the insertion process will be efficient, even at high temperature in the gas phase. The reaction will produce BO + CO in their ground states with the possibility of populating the first excited state of $BO(^2\Pi)$; $BO(^2\Pi)$ + CO ($^1\Sigma$) is calculated to be only 3.2 kcal/mol higher in energy than the B + CO_2 ground state.

The insertion product OBCO can be produced directly when hyperthermal boron atoms produced by laser ablation are used in matrix isolation experiments. In such conditions, the OBCO molecule is thermalized and trapped in argon matrix cages at 10 K. The fact that annealing the argon matrix at 18 K does not produce additional OBCO species is in agreement with the calculated energy barrier and proves that the observed OBCO species are produced in the gas phase (or on the surface of the argon matrix) before trapping. Reaction with hyperthermal boron atoms might also produce *trans*-BOCO (in a much smaller extent), but this latter species will rearrange readily to OBCO because the corresponding transition structure is only 3 kcal/mol above *trans*-BOCO and 24 kcal/mol below the reactant ground states. Moreover, OBCO is much more stable than *trans*-BOCO. This latter species was not observed in argon matrices, which is consistent with the calculated potential energy surface.

Acknowledgment. Y.H. gratefully acknowledges computational facilities provided by the intensive calculation pole M3PEC-MESOCENTRE of the University Bordeaux I-DRIMM (http://www.m3pec.u-bordeaux1.fr), financed by the Regional Council of Aquitaine and the French Ministry of Research and Technology and by the Pôle de Modélisation of the Institut des Sciences Moléculaires (ISM CNRS UMR 5255) at the University Bordeaux I.

Supporting Information Available: Detail of the IRC calculations for the B + $CO_2 \xrightarrow{TS4}$ OBCO path. Calculated rate constants for the B + $CO_2 \xrightarrow{TS4}$ OBCO path at different temperatures. This material is available free of charge via the Internet at http://pubs.acs.org.

References and Notes

(1) Braunstein, P.; Matt, D.; Nobel, D. *Chem. Rev.* **1988**, *88*, 747.
(2) Pandey, K. K. Coord. *Coord. Chem. Rev.* **1995**, *140*, 37.
(3) Gibson, D. H. *Chem. Rev.* **1996**, *96*, 2063.
(4) Mascetti, J.; Tranquille, M. *J. Phys. Chem.* **1988**, *92*, 2177.
(5) Gallan, F.; Fouassier, M.; Tranquille, M.; Mascetti, J.; Pápai, I. *J. Phys. Chem. A* **1997**, *101*, 2626.
(6) Pápai, I.; Mascetti, J.; Fournier, R. *J. Phys. Chem. A* **1997**, *101*, 4465.
(7) Zhou, M.; Liang, B.; Andrews, L. *J. Phys. Chem. A* **1999**, *103*, 2013.
(8) Zhou, M.; Andrews, L. *J. Phys. Chem. A* **1999**, *103*, 2066.
(9) Mascetti, J.; Gallan, F.; Pápai, I. *Coord. Chem. Rev.* **1999**, *190−192*, 557.
(10) Liang, B.; Andrews, L. *J. Phys. Chem. A* **2002**, *106*, 4042.
(11) Caballol, R.; Sanchez Marcos, E.; Barthelat, J. C. *J. Phys. Chem.* **1987**, *91*, 1328.
(12) Mebel, A. M.; Hwang, D.-Y. *J. Phys. Chem. A* **2000**, *104*, 11622.
(13) Mebel, A. M.; Hwang, D.-Y. *J. Chem. Phys.* **2002**, *116*, 5633.
(14) Hwang, D.-Y.; Mebel, A. M. *Chem. Phys. Lett.* **2002**, *357*, 51.
(15) Pápai, I.; Hannachi, Y.; Gwizdala, S.; Mascetti, J. *J. Phys. Chem. A* **2002**, *106*, 4181.
(16) Pápai, I.; Schubert, G.; Hannachi, Y.; Mascetti, J. *J. Phys. Chem. A* **2002**, *106*, 9551.
(17) Hannachi, Y.; Mascetti, J.; Stirling, A.; Pápai, I. *J. Phys. Chem. A* **2003**, *107*, 6708.

(18) Dobrogorskaya, Y.; Mascetti, J.; Pápai, I.; Hannachi, Y. *J. Phys. Chem. A* **2005**, *109*, 7932.
(19) Burkholder, T. R.; Andrews, L.; Bartlett, R. J. *J. Phys. Chem.* **1993**, *97*, 3500.
(20) Hassanzadeh, P.; Hannachi, Y.; Andrews, L. *J. Phys. Chem.* **1993**, *97*, 6418.
(21) Hannachi, Y.; Hassanzadeh, P.; Andrews, L. *J. Phys. Chem.* **1994**, *98*, 6950.
(22) Lanzisera, D. V.; Hassanzadeh, P.; Hannachi, Y.; Andrews, L. *J. Am. Chem. Soc.* **1997**, *119*, 12402.
(23) Andrews, L.; Lanzisera, D. V.; Hassanzadeh, P.; Hannachi, Y. *J. Phys. Chem. A* **1998**, *102*, 3259.
(24) Martin, J. M. L.; Taylor, P. R.; Yustein, J. T.; Burkholder, T. R.; Andrews, L. *J. Chem. Phys.* **1998**, *102*, 3259.
(25) Andrews, L.; Hassanzadeh, P.; Martin, J. M. L.; Taylor, P. R.; Yustein, J. T. J. *Phys. Chem.* **1993**, *102*, 5839.
(26) Balucani, N.; Asvany, O.; Lee, Y. T.; Kaiser, R. I.; Galland, N.; Rayez, M. T.; Hannachi, Y. *J. Comput. Chem.* **2001**, *22*, 1359.
(27) Sillars, D.; Kaiser, R. I.; Galland, N.; Hannachi, Y. *J. Phys. Chem. A* **2003**, *107*, 5149.
(28) Kaiser, R. I.; Balucani, N.; Galland, N.; Caralp, F.; Rayez, M. T.; Hannachi, Y. *Phys. Chem. Chem. Phys.* **2004**, *6*, 2205.
(29) Zhang, F.; Sun, H. L.; Chang, A. H. H.; Gu, X.; Kaiser, R. I. *J. Phys. Chem. A* **2007**, *111*, 13305.
(30) Bettinger, H. F.; Kaiser, R. I. *J. Phys. Chem. A* **2004**, *108*, 4576.
(31) Balucani, N.; Asvany, O.; Lee, Y. T.; Kaiser, R. I.; Galland, N.; Hannachi, Y. *J. Am. Chem. Soc.* **2000**, *122*, 11234.
(32) Zhang, F.; Gu, X.; Kaiser, R. I.; Bettinger, H. F. *Chem. Phys. Lett.* **2008**, *450*, 178.
(33) Zhang, F.; Guo, X.; Gu, X.; Kaiser, R. I. *Chem. Phys. Lett.* **2007**, *440*, 56.
(34) Zhang, F.; Kao, C. H.; Chang, A. H. H.; Gu, X.; Kaiser, R. I. *Chem. Phys. Chem.* **2008**, *9*, 95.
(35) Canosa, A.; Le Picard, S. D.; Geppert, W. D. *J. Phys. Chem. A* **2001**, *105*, 11549.
(36) Le Picard, S. D.; Canosa, A.; Geppert, W. D.; Stoecklin, T. *Chem. Phys. Lett.* **2004**, *385*, 502.
(37) Geppert, W. D.; Goulay, F.; Naulin, C.; Costes, M.; Canosa, A.; Le Picard, S. D.; Rowe, B. R. *Phys. Chem. Chem. Phys.* **2004**, *6*, 566.
(38) DiGiuseppe, T. G.; Davidovits, P. *J. Chem. Phys.* **1981**, *74*, 3287.
(39) Marshall, P.; O'Connor, P. B.; Chan, W.-T.; Kristof, P. V.; Goddard, J. D. In *Gas-Phase Metal Reactions*; Fontyn, A., Ed.; Elseviers: Amsterdam, 1992.
(40) Chin, C.-H.; Mebel, A. M.; Hwang, D.-Y. *Chem. Phys. Lett.* **2003**, *375*, 670.
(41) Frisch, M. J.; Trucks, G. W.; Schlegel, H. B.; Scuseria, G. E.; Robb, M. A.; Cheeseman, J. R.; Montgomery, J. A., Jr.; Vreven, T.; Kudin, K. N.; Burant, J. C.; Millam, J. M.; Iyengar, S. S.; Tomasi, J.; Barone, V.; Mennucci, B.; Cossi, M.; Scalmani, G.; Rega, N.; Petersson, G. A.; Nakatsuji, H.; Hada, M.; Ehara, M.; Toyota, K.; Fukuda, R.; Hasegawa, J.; Ishida, M.; Nakajima, T.; Honda, Y.; Kitao, O.; Nakai, H.; Klene, M.; Li, X.; Knox, J. E.; Hratchian, H. P.; Cross, J. B.; Bakken, V.; Adamo, C.; Jaramillo, J.; Gomperts, R.; Stratmann, R. E.; Yazyev, O.; Austin, A. J.; Cammi, R.; Pomelli, C.; Ochterski, J. W.; Ayala, P. Y.; Morokuma, K.; Voth, G. A.; Salvador, P.; Dannenberg, J. J.; Zakrzewski, V. G.; Dapprich, S.; Daniels, A. D.; Strain, M. C.; Farkas, O.; Malick, D. K.; Rabuck, A. D.; Raghavachari, K.; Foresman, J. B.; Ortiz, J. V.; Cui, Q.; Baboul, A. G.; Clifford, S.; Cioslowski, J.; Stefanov, B. B.; Liu, G.; Liashenko, A.; Piskorz, P.; Komaromi, I.; Martin, R. L.; Fox, D. J.; Keith, T.; Al-Laham, M. A.; Peng, C. Y.; Nanayakkara, A.; Challacombe, M.; Gill, P. M. W.; Johnson, B.; Chen, W.; Wong, M. W.; Gonzalez, C.; Pople, J. A. *Gaussian 03*, revision D.02; Gaussian, Inc.: Wallingford, CT, 2004.
(42) Becke, A. D. *J. Chem. Phys.* **1993**, *98*, 5648.
(43) Lee, C.; Yang, W.; Parr, R. G. *Phys. Rev. B* **1988**, *73*, 785.
(44) Stephens, P. J.; Devlin, F. J.; Chabalowski, C. F.; Frisch, M. J. *J. Phys. Chem.* **1994**, *98*, 11623.
(45) Dunning, T. H. *J. Chem. Phys.* **1989**, *90*, 1007.
(46) Kendall, R. A.; Dunning, T. H.; Harrison, R. J. *J. Chem. Phys.* **1992**, *96*, 6796.
(47) Purvis, G. D.; Bartlett, R. J. *J. Chem. Phys.* **1982**, *76*, 1910.
(48) Pople, J. A.; Head-Gordon, M.; Raghavachari, K. *J. Chem. Phys.* **1987**, *87*, 5968.
(49) Seeger, R.; Pople, J. A. *J. Chem. Phys.* **1977**, *66*, 3045.
(50) Bauernschmitt, R.; Ahlrichs, R. *J. Chem. Phys.* **1996**, *104*, 9047.
(51) Baboul, A. G.; Curtiss, L. A.; Redfern, P. C.; Raghavachari, K. *J. Chem. Phys.* **1999**, *110*, 7650.
(52) Gonzalez, C.; Schlegel, H. B. *J. Chem. Phys.* **1989**, *90*, 2154.
(53) Zhao, Y.; Truhlar, D. G. *J. Phys. Chem. A* **2004**, *108*, 6908.
(54) Hehre, W. J.; Ditchfield, R.; Pople, J. A. *J. Chem. Phys.* **1972**, *56*, 2257.
(55) Hehre, W. J.; Radom, L.; Schleyer, P. v. R.; Pople, J. A. *Ab Initio Molecular Orbital Theory*; Wiley: New York, 1986.
(56) Huber, K. P.; Herzberg, G. *Constants of Diatomic Molecules*; Van Nostrand Reinhold: New York, 1979.
(57) Herzberg, G. *Molecular Spectra and Molecular Structure III. Electronic Spectra and Electronic Structure of Polyatomic Molecules*; Van Nostrand Reinhold: New York, 1966.
(58) Chase, M. W., Jr.; Davies, C. A.; Downey, J. R., Jr.; Frurip, D. J.; McDonald, R. A.; Syverud, A. N. JANAF Tables, Third Edition, 3rd ed. *J. Phys. Chem. Ref. Data* 1985, 14. Suppl. 1.
(59) Pilling, M. J.; Seakins, P. W. *Reaction Kinetics*; Oxford University Press: Oxford, 1996.
(60) Ralchenko, Yu.; Kramida, A. E.; Reader, J.;NIST ASD Team (2008). NIST Atomic Spectra Database, version 3.1.4. Available at http://physics.nist.gov/asd3; National Institute of Standards and Technology: Gaithersburg, MD, 2008.

JP804504G